Hindawi
Geofluids
Volume 2021, Article ID 4029439, 10 pages
https://doi.org/10.1155/2021/4029439

Research Article

A Practical Design Method for Reducing Postconstruction Settlement of Highway Subgrade Induced by Soil Creep

Fei Zhou,[1] **Tangdai Xia**,[1] **Bingqi Yu**,[1] **Fan Xia**,[1] **and Fan Yu**[2]

[1]*Research Center of Coastal and Urban Geotechnical Engineering, Zhejiang University, Hangzhou 310058, China*
[2]*Zhejiang Provincial Institute of Communications Planning, Design & Research, Zhejiang, Hangzhou 310006, China*

Correspondence should be addressed to Tangdai Xia; xtd@zju.edu.cn

Received 10 September 2021; Accepted 15 October 2021; Published 5 November 2021

Academic Editor: Yu Wang

The postconstruction settlement of the bridge approach is usually uneven, which could create a bump in the roadway. Indeed, this is a typical situation at the end of the bridge approach and requires a solution. One of the main causes of postconstruction settlement is the creep of soil. This paper is aimed at generalizing a new design method for controlling highway postconstruction settlement by replacing subgrade with expanded polystyrene (EPS). In the new method, the creep coefficient can be calculated based on the Yin-Graham EVP model. Thus, the relationship between the overloading ratio (OLR) and overconsolidation ratio (OCR) is obtained. The new method involves five steps: (a) determine the creep coefficient based on the relationship between the creep coefficient and over consolidation ratio, (b) divide the ground into a suitable number of sublayers, (c) select groups of different overloading ratios and then calculate the average values of the additional stress and overconsolidation ratio for each sublayer under different OLRs, (d) calculate the postconstruction settlement under different OLRs, and (e) determine the replacement capacity for different sections. This method can be used for quantitative design according to different requirements of postconstruction settlement of foundation. Taking Huzhou Avenue as an example, the case study illustrates the calculation process of the new method in detail.

1. Introduction

The bridge approaches provide a smooth transition of cars from roadway pavements to bridge structures. However, the postconstruction settlement of bridge approaches is usually uneven, which could create a bump in the roadway. Indeed, this is a typical situation at the bridge approach and requires a solution.

The bump at bridge-head is a complicated technical problem. The creep of soil is one of the main causes of postconstruction settlement. The soil exhibits creep properties. Compared with primary consolidation settlement, creep settlement is small but significant, especially for soft clay. In the past several decades, extensive studies have been conducted on the creep of soft clay. Ladd et al. [1] first proposed the question of whether creep settlement occurs in the process of primary consolidation settlement. And there are two different views on whether the creep occurs during primary consolidation. They summed them up as Hypothesis A and Hypothesis B. Hypothesis A holds that creep occurs only in the secondary consolidation stage, and no creep occurs in the primary consolidation stage. Mesri et al. [2–4], Wang et al. [3], and Mesri and Vardhanabhuti [4] support Hypothesis A. However, Hypothesis B believes that the soil creep is caused by its own viscosity and occurs from the beginning of the primary consolidation process. It is supported by Bjerrum [5], Stolle et al. [6], Nash and Ryde [7], Yin et al. [8], Suklje [9], Bouchard et al. [10], Berre and Iversen [11], Leoni et al. [12], Karim et al. [13], and Nash and Brown [14]. As is known, with the effective stress changes, the creep always

exists actually, which means that Hypothesis B is reasonable. Based on Hypothesis B and the equivalent time concept, Yin and Graham [15–18] proposed a 1D elastic viscoplastic (EVP) model for creep behavior, which can be used to calculate the creep settlement. According to the EVP model, the creep coefficient is closely related to the over consolidation ratio (OCR).

Some compression tests [19–21] have shown that the creep coefficient decreases with the increase of OCR. Therefore, the use of a preload larger than the final construction load is an effective method to reduce postconstruction settlement [22–26]. However, in the actual project, for some sections, the preloading period is insufficient so that it is difficult to achieve the original effect within the time limit of the project. The method of replacing part of subgrade with lightweight materials to reduce the permanent load of subgrade can solve the problem [27, 28]. Expanded polystyrene (EPS) is one of the high-quality lightweight materials [29]. EPS has the characteristics of ultralightweight, compressibility resistance, self-reliance, water resistance, flame retardant, and so on. The density of the EPS material is generally $0.2 \sim 0.3\,\mathrm{kN/m^3}$, which is equivalent to 1/100~1/60 of the soil density. EPS has high compressive strength and varies with density, so it can be used as an embankment filling material in the elastic range of $80\sim140\,\mathrm{kN/m^2}$. EPS is a synthetic resin foam containing independent bubbles that do not absorb water. The physical properties and mechanical indexes of the EPS material change little in the aging process, excellent aging resistance, and its aging life is more than 60 years.

It is important to determine the appropriate thickness of EPS to control the postconstruction settlement but there are only few studies in this area. Chen et al. [30] suggest that consolidation, compression, and other parameters can be calculated according to the monitoring data, and the calculation program of foundation settlement reflecting the process of overloading-unloading and reloading should be compiled. Then, the relationship between different capacities of lightweight material and postconstruction settlement is obtained. Thus, the thickness of the lightweight material can be determined according to the allowable postconstruction settlement. Many factors are considered in this method, but it is difficult to be generalized and applied in engineering due to its complex calculation. Jiang et al. [31] come up with a formula to calculate the thickness. However, this formula also relies on monitoring data and the postconstruction settlement is only estimated according to the measured data. Therefore, this formula may not be used in the stage of design.

This paper is aimed at proposing a new practical design method for controlling highway postconstruction settlement by replacing subgrade with EPS. First, the functional relationship between the creep coefficient and overconsolidation ratio is established by fitting the one-dimensional compression test data. Second, the relationship between the overloading ratio (OLR) and overconsolidation ratio (OCR) is deduced. Then, groups of different OLR are selected and the postconstruction settlement under different OLRs is calculated. This method can be used for quantitative design according to different requirements of postconstruction settlement of foundation. And it can make the OLR greater than 1.3 without the limitation of foundation stability.

2. Creep Coefficient of Overconsolidated Soil

Buisman proposed the concept of secondary consolidation coefficient (C_α). As is shown in Figure 1, it is believed that the $e - \lg t$ curve is close to a straight line after primary consolidation. The slope of the straight line part i is defined as secondary consolidation coefficient C_α.

$$C_\alpha = \frac{e_0 - e_1}{\lg t_1 - \lg t_0}, \tag{1}$$

where t_0 is the time at the end of primary consolidation and t_1 is any time after the end of primary consolidation.

However, Equation (1) is not applicable to the overconsolidated soil because overconsolidated soil has finished primary consolidation before test. In 1964, Crawford [32] conducted normally consolidated soil compressive rheological tests and plotted $e - \lg p$ curves of different consolidation times. In 1967, Bjerrum made a creep diagram. As is shown in Figure 2, he divided the displacements which he observed in the actual engineering into "instant compression" and "delayed compression" and proposed that the delayed compression can be described with parallel lines in $e - \lg \sigma$ space.

Based on Bjerrum's creep diagram, Yin-Graham proposed the 1-D EVP model, and the total strains can be written as follows:

$$\varepsilon_z = \varepsilon_{zo} + \frac{\lambda}{V} \ln\left(\frac{\sigma_z'}{\sigma_{zo}'}\right) + \frac{\psi}{V} \ln\left(\frac{t_e + t_o}{t_o}\right), \tag{2}$$

where ε_{zo} is a reference strain and ε_z is the total strain. σ_{zo}' is a reference stress that corresponds, respectively, to the strain at the beginning of loading. For normally consolidated soil, σ_{zo}' corresponds to strain ε_{zo}. V is the specific volume of the soil $(1 + e)$, that is, the volume occupied by unit volume of solids. So $\lambda = C_c/2.303$ and $\psi = C_{\alpha e}/2.303$, where C_c and $C_{\alpha e}$ are the compression index and creep coefficient under logarithmic coordinates. Here, we call $C_{\alpha e}$ "creep coefficient" instead of the "secondary consolidation coefficient", because Equation (2) considers creep occurs during and after "primary consolidation." And t_o is a parameter that can be measured by one-dimensional compression test, which is usually taken as unit time or the boundary point between the primary consolidation and secondary consolidation [33]. t_e is called the equivalent time as defined by Yin and Graham.

According to Equation (2), the void ratio e, the effective stress σ, and the equivalent t_e have a unique relationship.

$$e = e_o - C_c \lg\left(\frac{\sigma_z'}{\sigma_{zo}'}\right) - C_{\alpha e} \lg\left(\frac{t_e + t_o}{t_o}\right). \tag{3}$$

As is shown in Figure 3, no matter if it is normal consolidation soil or overconsolidated soil, the zero point of time is taken as the loading start time of its corresponding normal

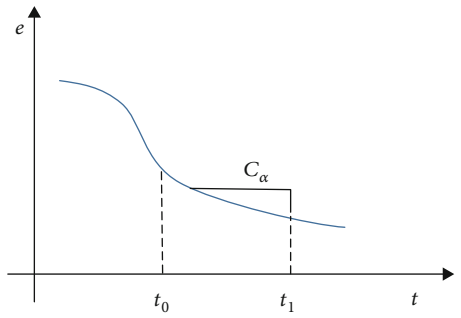

Figure 1: Primary consolidation and secondary consolidation of normally consolidated soil.

consolidation condition. For example, point 2 in Figure 3 is under overconsolidation condition, and its corresponding normal consolidation condition is point 5 on the normal consolidation line. The time corresponding to point 5 is the beginning time. And t_e is the equivalent time that is from point 5 to point 2. Such a time coordinate system combines normal consolidation and overconsolidation into a unified time coordinate system, so it is called an absolute time coordinate system. Now, t_e can be found from

$$C_{\alpha e0} \lg\left(\frac{t_e + t_o}{t_o}\right) = (C_c - C_e) \lg\left(\frac{\sigma'_z}{\sigma'_{zo}}\right), \tag{4}$$

where $C_{\alpha e0}$ is the normal consolidation soil creep coefficient and C_e is the expansion coefficient. From which

$$t_e = t_o\left(\frac{\sigma'_z}{\sigma'_{zo}}\right)^{(C_c - C_s)/C_{\alpha eo}} - t_o. \tag{5}$$

Let

$$\mathrm{OCR} = \frac{\sigma'_z}{\sigma'_{zo}}, \quad \delta = \frac{C_c - C_s}{C_{\alpha eo}}. \tag{6}$$

t_e can be expressed as follows:

$$t_e = t_o(\mathrm{OCR})^{\delta} - t_o. \tag{7}$$

According to Equation (7), t_e is a parameter related to OCR, and it can reflect the stress history and the state of soil. For overconsolidated soil, the creep coefficient of overconsolidated soils can be expressed as

$$\begin{aligned} C_{\alpha e} &= \frac{e_1 - e_2}{\lg\left((t_{e2} + t_o)/(t_{e1} + t_o)\right)} \\ &= \frac{e_1 - e_2}{\lg\left((t_{e1} + \Delta t + t_o)/(t_{e1} + t_o)\right)} \\ &= \frac{e_1 - e_2}{\lg\left(1 + (\Delta t/(t_{e1} + t_o))\right)}, \end{aligned} \tag{8}$$

where t_{e1} and t_{e2} are the equivalent time; e_1 and e_2 are the void ratios at equivalent time t_{e1} and t_{e2}, respectively; and $\triangle t$ is the current load duration from t_{e1} to t_{e2}.

According to Equations (7) and (8), the creep coefficient is not a constant. It can be expressed as a function with overconsolidation ratio.

$$C_{\alpha e} = f(\mathrm{OCR}). \tag{9}$$

3. The Relationship between Overconsolidation Ratio (OCR) and Overloading Ratio (OLR)

The maximum value of load in the past, namely, the preload, divided by the present value of load, is defined as the overload ratio (OLR). Overload ratio (OLR) was proposed to reflect overload state, which can be expressed as follows:

$$\mathrm{OLR} = \frac{p_o}{p_f}, \tag{10}$$

where p_o is the preload, that is, the load under the condition of overload preloading. p_f is the present value of load, that is, the final construction load on the ground surface.

The maximum value of effective stress in the past, namely, the preconsolidation pressure, divided by the present value of effective value of effective stress, is defined as the overconsolidation ratio (OCR).

$$\mathrm{OCR} = \frac{\sigma_c}{\sigma_0}, \tag{11}$$

where σ_o is the present effective stress and σ_c is the preconsolidation pressure.

When the load on the ground surface changes, the stress state of each point in the soil stratum will change, and OCR will also change. For example, as is shown in Figure 4, point A is under normal consolidation condition before loading. That is, σ_o is equal to $\gamma_i z$.

In soil mechanics, when load p_o is applied to the ground surface, the vertical additional stress σ_m is equal to αp_o. Here, α is the additional stress coefficient which can be calculated based on the depth of soil and the load distribution type. It is convenient that we can look up the additional stress coefficient table to determine its value. And when final load p_f is applied to the ground surface, the vertical additional stress σ_f is equal to αp_f. So, the OCR of point A can be expressed as follows:

$$\mathrm{OCR} = \frac{\sigma_o + \sigma_m}{\sigma_o + \sigma_f} = \frac{\gamma_i z + \alpha p_o}{\gamma_i z + \alpha p_f}. \tag{12}$$

As is shown in Figure 4,

$$H = h + \Delta h + h_s, \tag{13}$$

$$p_f = \gamma h + \gamma_E \Delta h + \gamma_s h_s, \tag{14}$$

$$p_o = \gamma H = \gamma(h + \Delta h + h_s), \tag{15}$$

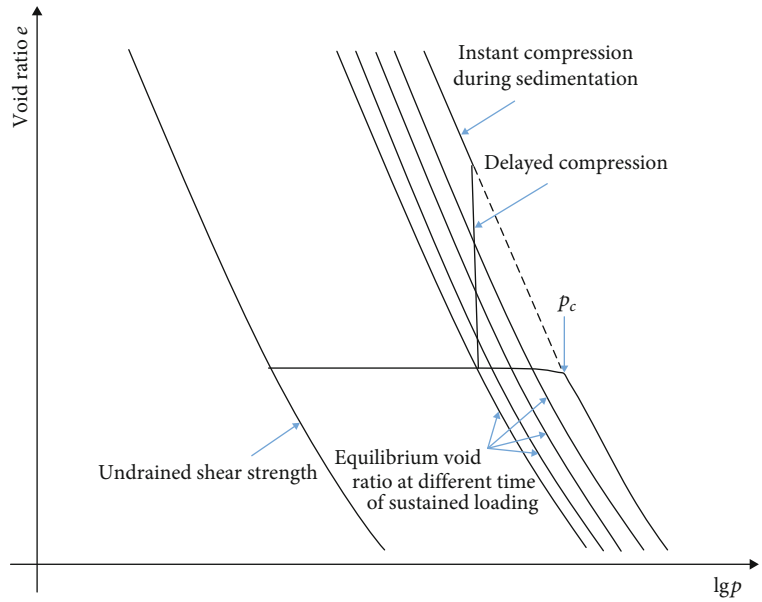

Figure 2: Bjerrum's creep diagram.

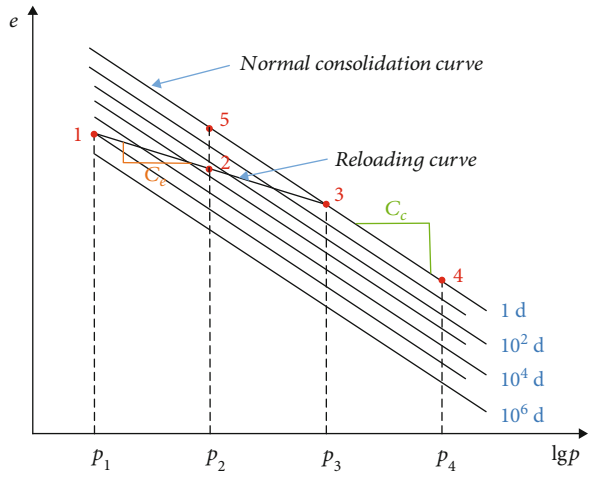

Figure 3: Equitime e – lg p curves.

where γ, γ_E, γ_i, and γ_s indicate the unit weight of filling soil, EPS, soft soil, and pavement, respectively; h, $\triangle h$, and h_s-indicate the thickness of soft soil, EPS, and pavement, respectively; and H is the designed height of embankment fill.

Let us establish the relationship between the OCR and OLR. Based on Equations (10) and (11),

$$\begin{aligned}\mathrm{OCR} &= \frac{\gamma_i z + \alpha\gamma(h+\Delta h+h_s)}{\gamma_i z + \alpha(\gamma h+\gamma_E\Delta h+\gamma_s h_s)}\\ &= \frac{\gamma_i z + \alpha\gamma h + \alpha(\gamma_E+(\gamma-\gamma_E))\Delta h + \alpha(\gamma_s+(\gamma-\gamma_s))h_s}{\gamma z + \alpha(\gamma h+\gamma_E\Delta h+\gamma_s h_s)}\\ &= 1+\frac{(\gamma-\gamma_E)\Delta h+(\gamma-\gamma_s)h_s}{\gamma h+\gamma_E\Delta h+\gamma_s h_s+(\gamma_i z/\alpha)},\end{aligned} \tag{16}$$

$$\begin{aligned}\mathrm{OLR} &= \frac{\gamma(h+\Delta h+h_s)}{\gamma h+\gamma_E\Delta h+\gamma_s h_s}\\ &= \frac{\gamma h+(\gamma_E+(\gamma-\gamma_E))\Delta h+(\gamma_s+(\gamma-\gamma_s))h_s}{\gamma h+\gamma_E\Delta h+\gamma_s h_s}\\ &= 1+\frac{(\gamma-\gamma_E)\Delta h+(\gamma-\gamma_s)h_s}{\gamma h+\gamma_E\Delta h+\gamma_s h_s}.\end{aligned} \tag{17}$$

According to Equations (14) and (15).

$$\frac{1}{\mathrm{OCR}-1}-\frac{1}{\mathrm{OLR}-1}=\frac{\gamma_i z}{\alpha(\gamma-\gamma_E)\Delta h+(\gamma-\gamma_s)h_s}. \tag{18}$$

Let

$$\beta(z)=\frac{\gamma_i z}{\alpha(\gamma-\gamma_E)\Delta h+(\gamma-\gamma_s)h_s}. \tag{19}$$

Thus, OCR, OLR, and z have a relationship:

$$\mathrm{OCR}=1+\frac{1}{(1/(\mathrm{OLR}-1))+\beta(z)}. \tag{20}$$

4. The New Method for Controlling Postconstruction Settlement

4.1. Procedures of Applying the Practical Design Method. The new method for controlling postconstruction settlement involves the following 5 steps:

(a) Determine the creep coefficient. Based on the Yin-Graham EVP model, the functional relationship between the creep coefficient and overconsolidation ratio is established by fitting the one-dimensional compression test data

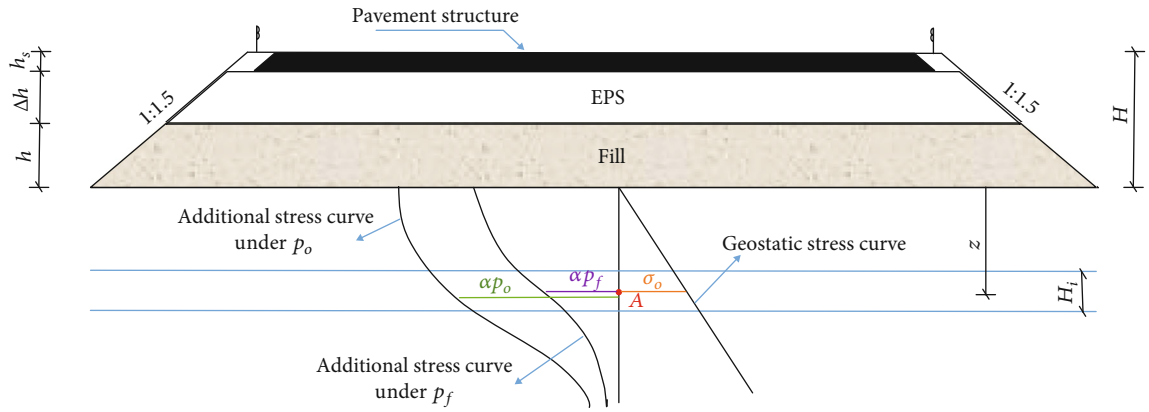

Figure 4: Cross-section of EPS filling.

(b) Divided the ground into a suitable number of sublayers. Each sublayer within a same soil layer should not be overly thick. The thickness of each sublayer should be controlled within 2 m-4 m. For each sublayer, it is assumed that pressure is uniformly distributed

(c) Select groups of different OLRs and calculate the average values of the additional stress and OCR for each sublayer under different OLRs. The OLR usually ranges from 1.1 to 1.6 in actual projects. Based on Equation (19), the additional stress and OCR at the center point of each sublayer are calculated and the values are taken as the average additional stress and OCR for each sublayer

(d) Calculate the postconstruction settlement under different OLRs. Based on the functional relationship between $C_{\alpha e}$ and OCR, the creep coefficient of each layer is determined according to the average overconsolidation ratio for each sublayer. According to Equation (20), the settlement of each sublayer was calculated and the total postconstruction settlement of ground can be calculated as follows:

$$s = \sum_{i=1}^{n} \frac{H_i}{1 + e_{oi}} C_{\alpha ei} \lg\left(\frac{t_1 + \Delta t}{t_1}\right), \tag{21}$$

where s is the total postconstruction settlement of ground, H_i is the thickness of each sublayer, $C_{\alpha ei}$ is the creep coefficient of each sublayer, t_1 is the preloading period, and Δt is the service period which is usually taken as 15 years

(e) Correct the settlement value with the safety factor μ and determine the overload ratio and the replacement capacity under the requirements of postconstruction settlement

4.2. Advantages of the New Method. On the one hand, the subgrade soils become overconsolidated soil after replacement with EPS, so the creep coefficient is greatly reduced. As a lightweight material, EPS itself has the characteristics of ultralightweight, compressibility resistance, self-reliance, water resistance, flame retardant, and so on. Therefore, this method can better control the postconstruction settlement.

On the other hand, this method can be used for the quantitative design according to different requirements of postconstruction settlement of foundation. In the process of the engineering design, the calculation of postconstruction settlement is often calculated by empirical formula or correction coefficient. This is often unable to meet the strict requirements of some engineering. Using the creep coefficient, this method can realize the quantitative calculation of postconstruction settlement.

Besides, this method can make the overloading ratio greater than 1.3 without the limitation of foundation stability. It is necessary to control the overloading ratio to ensure the stability of the foundation when using the overload preloading method for ground treatment. Thus, when the overloading is relatively small, a longer preloading time is needed to ensure the effect of controlling the postconstruction settlement, which would prolong the construction period. This method can make the overloading ratio greater than 1.3, which is like a strategy using space to exchange for time.

5. Case Study

5.1. Project Background. The considered Huzhou Avenue is constructed on soft clay on the Huzhou plain, southeast of the city of Huzhou in China. As is shown in Figure 5, the bridge approach is about 140 m long, which is divided into 5 transition sections (S1 to S5) and 1 general section (GS). The soft clay beneath it is about 13 m deep. In order to provide a smooth transition of vehicles from highway pavements to bridge structures, the design scheme is different for each section. Cement-soil mixed piles are used in S1 and S2. EPS lightweight materials are used in S3, S4, and S5. The plastic drainage plate is used in all sections.

The soft clay has high water content, a high void ratio, high compressibility, low strength, and low permeability. The soil profile is depicted in Figure 6, obtained from geological survey. The soil consists of 2 layers: (a) hard crust and (b) soft clay.

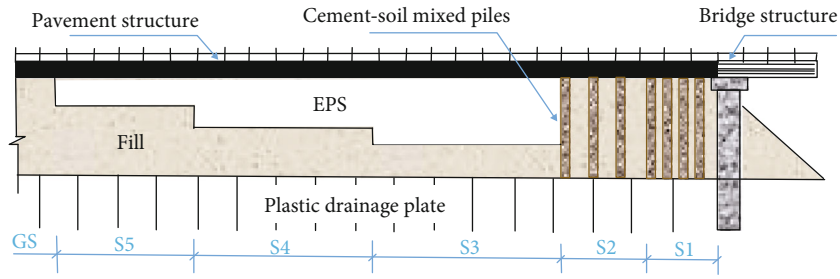

Figure 5: Profile of bridge approach.

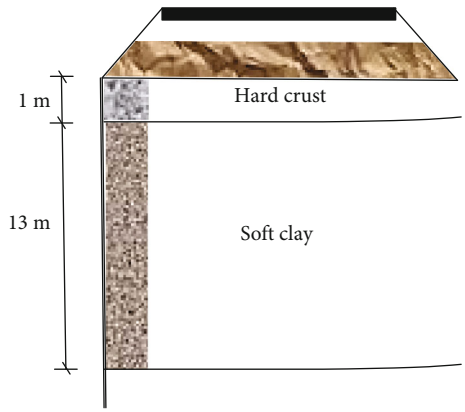

Figure 6: Profile of soil.

5.2. One-Dimensional Compression Test

5.2.1. Test Apparatus. As is shown in Figure 7, the sixteen automatic pneumatic consolidation apparatus is adopted to carry out one-dimensional compression test. The ring knife is 2 cm high, and the base area is 45.6 cm^2. Compared with traditional apparatus, the system has the advantage of automatic data acquisition during the test and overcomes the disadvantages of traditional manual recording. In order to ensure the reliability of the test results, the apparatus was proofread before the test.

5.2.2. Test Scheme and Description. In order to determine the stress history of the ground soils, the preconsolidation pressure should be first determined. Casagrande proposed an empirical graphical method using the $e - \lg p$ curve to obtain the maximum effective stress that had acted on the clay in the past. It is known through tests that the soft clay belongs to normally consolidated soil. The sample soils are taken from a depth of 5 m, and the preconsolidation pressure is about 110 kPa. In order to ensure that the maximum load is greater than the preconsolidation pressure, it is set as 150 kPa. The test loading path is divided into overloading, unloading, and reloading in order to simulate the actual construction condition. The soft clay is overconsolidated after reloading. For excluding the influence of the loading ratio factor, the loading ratio of each group is set as 1. Since the overconsolidation ratio is small and the creep coefficient changes greatly, the overconsolidation ratios are set as 1.1, 1.2, 1.4, and 1.8. It takes a long time for the creep coefficient to stabilize, so the duration of the last stage test should be at least 7 d. The specific scheme for one-dimensional compression tests is shown in Table 1.

5.2.3. Test Results. Figure 8 shows the $s - \lg t$ curve of sample 1. Since the sample soil belongs to normally consolidated soil, it is obvious that the boundary between the primary and secondary consolidations is at about $t_o = 100$ min. According to Equation (1),

$$C_\alpha = \frac{e_0 - e_1}{\lg t_1 - \lg t_0} = \frac{1.469 - 1.437}{\lg 1440 - \lg 100} = 0.0271. \tag{22}$$

Figure 9 shows the $e - \lg t$ curve of soil sample 2, sample 3, sample 4, and sample 5 under the last stage load. From Figure 9, we can learn that the lines of all samples are smooth after 100 min, so t_o is 100 min. And the duration should be reduced by 100 minutes, so $\triangle t = 7\text{d} - 100$ min $= 9980$ min. Since each stage of load, except the last stage, lasts for 1 day, the equivalent time should be taken as 1 day. According to Equation (8), the creep coefficient can be calculated.

Taking sample 2 as an example, $t_e = 1\text{d} = 1440$ min, $t_o = 100$ min, $\triangle t = 9980$ min, $e_1 = 1.245$, and $e_2 = 1.228$. So, when OCR is 1.1, the creep coefficient.

$$\begin{aligned} C_{\alpha e} &= \frac{e_1 - e_2}{\lg\left(1 + \left(\Delta t/\left(t_{e1} + t_o\right)\right)\right)} \\ &= \frac{1.245 - 1.228}{\lg\left(1 + \left(9980/\left(1440 + 100\right)\right)\right)} \\ &\approx 0.0197. \end{aligned} \tag{23}$$

The creep coefficients under each overconsolidation ratio are calculated as shown in Table 2.

The relationship between the creep coefficient and OCR is depicted in Figure 10.

It is found that the relationship between the creep coefficient and overconsolidation ratio can be fitted by an exponential function as follows, and the correlation coefficient R^2 is 0.991.

$$C_{\alpha e} = -0.0031 + 0.2446e^{-2.1184\text{OCR}}. \tag{24}$$

5.3. Calculate the Postconstruction Settlement. As is shown in Figure 11, to facilitate the analysis, it is assumed that p_o is divided into 2 stages that are abruptly applied on the ground

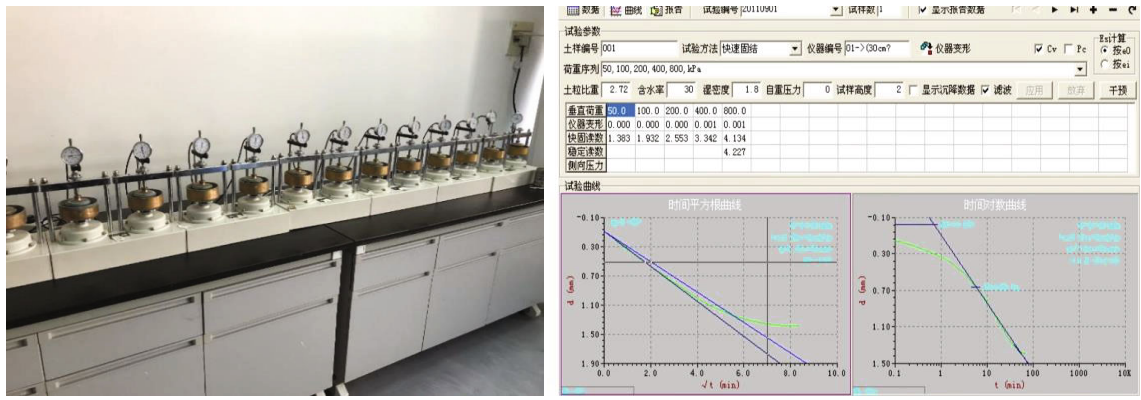

Figure 7: Automatic consolidation apparatus.

Table 1: Scheme for one-dimensional compression tests.

Sample	OCR	Load path and duration
1	1.0	37.5 kPa (1 d) ⟶75 kPa (1 d) ⟶150 kPa (7 d)
2	1.1	37.5 kPa (1 d) ⟶75 kPa (1 d) ⟶150 kPa (1 d) ⟶60.6 kPa (1 d) ⟶90.9 kPa (1 d) ⟶136.4 kPa (7 d)
3	1.2	37.5 kPa (1 d) ⟶75 kPa (1 d) ⟶150 kPa (1 d) ⟶55.5 kPa (1 d) ⟶83.33 kPa (1 d) ⟶125 kPa (7 d)
4	1.4	37.5 kPa (1 d) ⟶75 kPa (1 d) ⟶150 kPa (1 d) ⟶47.5 kPa (1 d) ⟶71.3 kPa (1 d) ⟶107 kPa (7 d)
5	1.8	37.5 kPa (1 d) ⟶75 kPa (1 d) ⟶150 kPa (1 d) ⟶37.0 kPa (1 d) ⟶55.5 kPa (1 d) ⟶ 83.3 kPa (7 d)

Note: the arrow direction in the loading path represents the next level stress. The number before the brackets is the value of the load, and the number in the brackets is the duration of the load. For example, 37.5 kPa (1 d) represents that the load is 37.5 kPa (duration is 1 day).

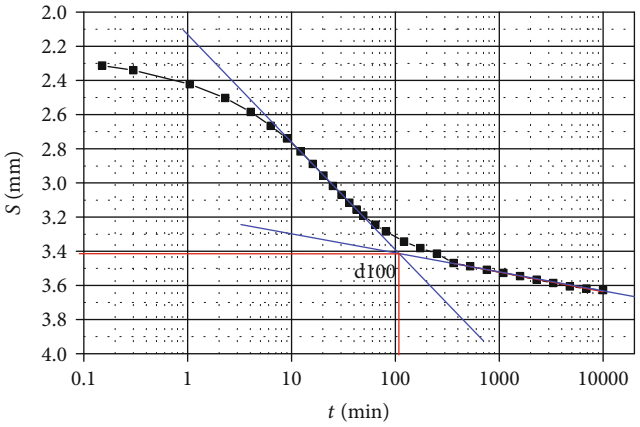

Figure 8: $s - \lg t$ curve.

surface. When the final stage is applied up to t_2, the additional surcharge is replaced with lightweight EPS, and the preload is reduced from p_o to p_m. And then, the pavement is laid and the load is up to p_f.

As is shown in Figure 6, the thickness of hard crust is approximate 1 m. Due to its low compressibility, the post-construction settlement of this layer is negligible. The designed height of embankment fill H is 4.4 m. The unit weight of filling soil γ is taken as 20 kN/m^3. According to Equation (13),

$$p_o = \gamma H = 20 \times 4.4 = 88 \text{ kPa}. \tag{25}$$

The designed thickness of pavement structure layer h_s is 0.9 m. And its unit weight γ_s is taken as 23 kN/m^3. When the thickness of EPS $\triangle h$ is taken as 0.5 m, according to Equations (13) and (15), the final load p_f and OLR are calculated below.

$$\begin{aligned} p_f &= \gamma h + \gamma_E \Delta h + \gamma_s h_s \\ &= 20 \times 3 + 0.2 \times 0.5 + 23 \times 0.9 \\ &= 80.47 \text{ kPa}, \end{aligned} \tag{26}$$

$$\text{OLR} = \frac{p_o}{p_f} = \frac{88}{80.47} = 1.093. \tag{27}$$

For the first soil layer, the depth of the middle point $z = 1$ m. Having looking up the additional stress coefficient table, we obtain $\alpha = 1.0$. According to Equations (18), (19), and (21),

$$\begin{aligned} \beta(z) &= \frac{\gamma_i z}{\alpha(\gamma - \gamma_E)\Delta h + (\gamma - \gamma_s)h_s} \\ &= \frac{16 \times 1}{1 \times (20 - 0.3) \times 0.5 + (20 - 23) \times 0.9} \\ &= 1.838, \end{aligned} \tag{28}$$

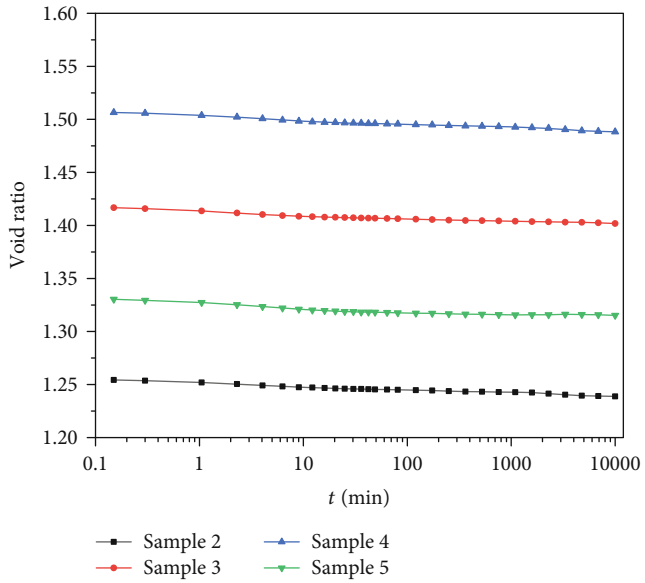

Figure 9: $e - \lg t$ curve of overconsolidated soil.

Table 2: Creep coefficient under different OCRs.

OCR	$C_{\alpha e}$
1.0	0.0271
1.1	0.0197
1.2	0.0156
1.4	0.0107
1.8	0.0019

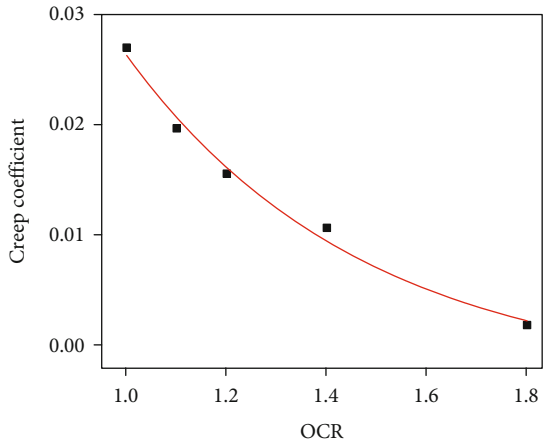

Figure 10: The relationship between the creep coefficient and OCR.

$$\begin{aligned} \mathrm{OCR} &= 1 + \frac{1}{(1/(\mathrm{OLR} - 1)) + \beta(z)} \\ &= 1 + \frac{1}{(1/(1.093 - 1)) + 1.838} \\ &= 1.077, \end{aligned} \tag{29}$$

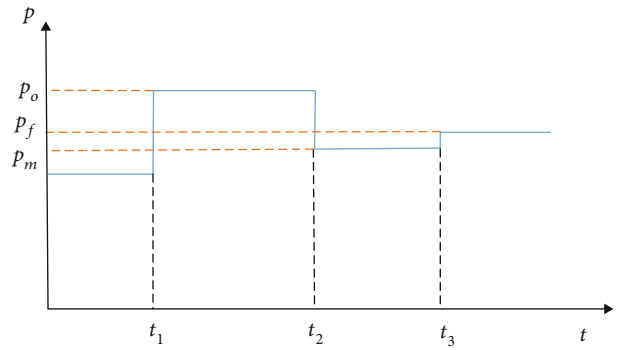

Figure 11: Schematic diagram of load-time.

$$C_{\alpha e} = -0.0031 + 0.2446e^{-2.1184\mathrm{OCR}} = 0.0227. \tag{30}$$

In this project, the timing of replacement is the timing of unloading. As the timing of unloading is mainly determined based on the degree of primary consolidation, the timing of replacement could be determined with traditional method. The preloading period lasts 1 year, so $t_1 = 1$ year. The postconstruction settlement at the end of the service period can be calculated according to Equation (19).

$$\begin{aligned} s_1 &= \frac{H_1}{1 + e_o} C_{\alpha e} \lg\left(\frac{t_1 + \Delta t}{t_1}\right) \\ &= \frac{2}{1 + 1.574} \times 0.0227 \lg\left(\frac{1 + 15}{1}\right) \\ &= 0.021\mathrm{m}. \end{aligned} \tag{31}$$

The postconstruction settlement of other soil layers is calculated in turn, and the calculation results are shown in Table 3.

Actually, the degree of consolidation cannot reach 100%, so the calculated postconstruction settlement should be corrected. The correction factor μ can be evaluated according to the degree of consolidation. The correction factor μ is an empirical coefficient. Here, according to existing engineering experience, as is shown in Table 4, we suggest the value of the correction factor should be determined based on the degree of consolidation after preloading. In this project, the degree of consolidation after preloading is about 80%, so the correction coefficient is 1.3.

According to the above calculation process, the postconstruction settlement under different OLRs is calculated as Table 5.

The allowable postconstruction settlement of the general section is 30 cm, which is the requirement in the specification. The longitudinal grade allowable value is 4‰. As is shown in Figure 5, the distance between the general section and Section 3 is 65 m. If the OLR of Section 3 is set as 1.09, the longitudinal grade is $(300 - 141.7)/65000 = 2.4‰ < 4‰$.

As is shown in Figure 12, the settlement curve of the cross-section is distributed in parabolic shape roughly. However, the calculated overloading ratio above is that of the

Table 3: Settlement calculation results.

i	H_i	α	β	OCR	$C_{\alpha e}$	s
1	2(1.0)	1	4.900	1.062	0.0227	0.021
2	3(4.5)	1	7.351	1.054	0.0231	0.032
3	2(7.0)	0.95	18.054	1.034	0.0242	0.023
4	2(9.0)	0.93	23.712	1.028	0.0245	0.023
5	2(11.0)	0.89	30.284	1.024	0.0248	0.023
6	2(13.0)	0.86	37.038	1.020	0.0251	0.023
Sum						0.145

Note: the number in parenthesis is the depth of the middle of each layer.

Table 4: Correction factor.

The degree of consolidation	μ
>95%	1.1
85% ~ 95%	1.2
75% ~ 85%	1.3
<75%	1.4

$[s] = \mu \times s = 1.3 \times 145 = 188.5$ mm.

Table 5: Postconstruction settlement under different OLRs.

$\triangle h$	OLR	s (mm)	$[s]$ (mm)
0.5	1.09	145	188.5
1.0	1.25	126	163.8
1.5	1.45	109	141.7

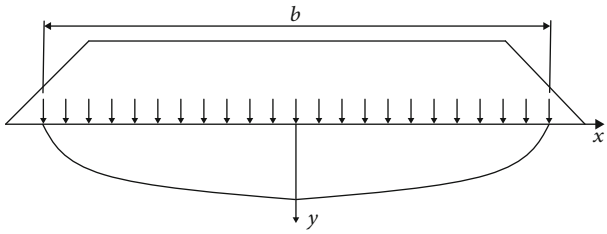

Figure 12: Settlement curve of cross-section of embankment.

midpoint of each section. So, the cross-section can be optimized to get more economical. The specific optimization content will be introduced in another article.

6. Conclusions

Based on practical engineering, a new design method for controlling postconstruction settlement is proposed in this paper. Main conclusions are drawn as follows:

(a) Based on the1D EVP model and the concept of equivalent time, the functional relationship between the creep coefficient and overconsolidation ratio can be established by fitting one-dimensional compression test data. It is found that the creep coefficient decreases with the overconsolidation ratio increasing

(b) The relationship between the overloading ratio and overconsolidation ratio is deduced. In practical engineering, the overconsolidation ratio can be changed by adjusting the overloading ratio, and then, the creep coefficient can be changed to control the postconstruction settlement

(c) The new method can be used for the quantitative design according to different requirements of postconstruction settlement of foundation. The case study shows that the method is operable in engineering

Data Availability

The data used to support the findings of this study are available from the corresponding author upon request.

Conflicts of Interest

The authors declare that there are no conflicts of interest regarding the publication of this paper.

References

[1] C. C. Ladd, R. Foott, K. Ishihara, F. Schlosser, and H. G. Poulos, "Stress–deformation and strength characteristics," in *State of the Art Report, 9th International Conference on Soil Mechanics and Foundation Engineering*, 1977.

[2] G. Mesri, "Effects of friction and thickness on long-term consolidation behavior of Osaka Bay Clays[1]," *Soils and Foundations*, vol. 49, no. 5, pp. 823-824, 2009.

[3] Y. Wang, Y. F. Yi, C. H. Li, and J. Q. Han, "Anisotropic fracture and energy characteristics of a Tibet marble exposed to multi-level constant-amplitude (MLCA) cyclic loads: a lab-scale testing," *Engineering Fracture Mechanics*, vol. 244, p. 107550, 2021.

[4] G. Mesri and B. Vardhanabhuti, "Closure to "secondary compression" by G. Mesri and B. Vardhanabhuti," *Journal of Geotechnical and Geoenviromental Engineering*, vol. 132, no. 6, pp. 817-818, 2006.

[5] L. Bjerrum, "Engineering geology of Norwegian normally-consolidated marine clays as related to settlements of buildings," *Géotechnique*, vol. 17, no. 2, pp. 83–118, 1967.

[6] D. Stolle, P. A. Vermeer, and P. G. Bonnier, "A consolidation model for a creeping clay," *Canadian Geotechnical Journal*, vol. 36, no. 4, pp. 754–759, 1999.

[7] D. Nash and S. J. Ryde, "Modelling consolidation accelerated by vertical drains in soils subject to creep," *Géotechnique*, vol. 51, no. 3, pp. 257–273, 2001.

[8] J.-H. Yin, J.-G. Zhu, and J. Graham, "A new elastic visco-plastic model for time-dependent behaviour of normally and over-consolidated clays: theory and verification," *Canadian Geotechnical Journal*, vol. 39, no. 1, pp. 157–173, 2002.

[9] L. Suklje, "On some controversial effects of the viscous structural resistance of soil," *Acta Geotechnica*, vol. 84, pp. 1–25, 1982.

[10] R. Bouchard, F. Tavenas, M. Kabbaj, and S. Leroueil, "Stress–strain–strain rate relation for the compressibility of sensitive natural clays," *Géotechnique*, vol. 35, no. 2, pp. 159–180, 1985.

[11] T. Berre and K. Iversen, "Oedometer test with different specimen heights on a clay exhibiting large secondary compression," *Géotechnique*, vol. 22, no. 1, pp. 53–70, 1972.

[12] M. Leoni, M. Karstunen, and P. A. Vermeer, "Anisotropic creep model for soft soils," *Géotechnique*, vol. 58, no. 3, pp. 215–226, 2008.

[13] M. R. Karim, C. T. Gnanendran, S.-C. R. Lo, and J. Mak, "Predicting the long-term performance of a wide embankment on soft soil using an elastic viscoplastic model," *Canadian Geotechnical Journal*, vol. 47, no. 2, pp. 244–257, 2010.

[14] D. Nash and M. Brown, "Influence of destructuration of soft clay on time-dependent settlements: comparison of some elastic viscoplastic models," *International Journal of Geomechanics*, vol. 15, no. 5, 2015.

[15] J. H. Yin and J. Graham, "Viscous-elastic-plastic modelling of one-dimensional time-dependent behaviour of clays," *Canadian Geotechnical Journal*, vol. 26, no. 2, pp. 199–209, 1989.

[16] Y. Wang, B. Zhang, B. Li, and C. H. Li, "A strain-based fatigue damage model for naturally fractured marble subjected to freeze-thaw and uniaxial cyclic loads," *International journal of damage mechanics*, vol. 6, 2021.

[17] J. H. Yin and J. Graham, "Equivalent times and one-dimensional elastic viscoplastic modelling of time-dependent stress-strain behaviour of clays," *Canadian Geotechnical Journal*, vol. 31, no. 1, pp. 42–52, 1994.

[18] J. H. Yin, "Non-linear creep of soils in oedometer tests," *Géotechnique*, vol. 49, no. 5, pp. 699–707, 1999.

[19] W.-Q. Feng and J.-H. Yin, "A new simplified hypothesis b method for calculating consolidation settlements of double soil layers exhibiting creep," *International Journal for Numerical and Analytical Methods in Geomechanics*, vol. 41, no. 6, pp. 899–917, 2017.

[20] Y. Wang, C. H. Li, and J. Q. Han, "On the effect of stress amplitude on fracture and energy evolution of pre- flawed granite under uniaxial increasing-amplitude fatigue loads," *Engineering Fracture Mechanics*, vol. 240, p. 107366, 2020.

[21] Y.-Y. Hu, W.-H. Zhou, and Y.-Q. Cai, "Large-strain elastic viscoplastic consolidation analysis of very soft clay layers with vertical drains under preloading," *Canadian Geotechnical Journal*, vol. 51, no. 2, pp. 144–157, 2014.

[22] S. J. Johnson, "Precompression for improving foundation soil," *Soil Mechanics and Foundation Division Journal*, vol. 96, no. 1, 1970.

[23] Y. Wang, W. K. Feng, H. J. Wang, C. H. Li, and Z. Q. Hou, "Rock bridge fracturing characteristics in granite induced by freeze-thaw and uniaxial deformation revealed by AE monitoring and post-test CT scanning," *Cold Regions Science and Technology*, vol. 177, p. 103115, 2020.

[24] A. C. Stamatopoulos and P. C. Kotzais, "Settlement-time predictions in preloading," *Journal of Geotechnical Engineering*, vol. 109, no. 6, pp. 807–820, 1983.

[25] Y. Y. Hu, "Particular behaviors of quasi-plastic viscous elastic model under consolidation," *International Journal of Geomechanics*, vol. 16, no. 4, pp. 04016003–04016018, 2016.

[26] G. W. Li, T. Yang, and Z. Z. Yin, "Study of mechanism about surcharge preloading method on the soft ground of highways," *Chinese Journal of Geotechnical Engineering*, vol. 28, no. 7, pp. 896–901, 2006.

[27] S. Saride, A. J. Puppala, R. Williammee, and S. K. Sirigiripet, "Use of lightweight ECS as a fill material to control approach embankment settlements," *Journal of Materials in Civil Engineering*, vol. 22, no. 6, pp. 607–617, 2010.

[28] S. V. Deijk, "A review of the Netherlands approach to the use of foam concrete in Holland and at canary wharf," *Concrete*, vol. 25, no. 5, pp. 49–54, 1991.

[29] D. J. Thompsett, A. Walker, R. J. Radley, and B. M. Grieveson, "Design and construction of expanded polystyrene embankments: practical design methods as used in the United Kingdom," *Construction and Building Materials*, vol. 9, no. 6, pp. 403–411, 1995.

[30] Y. H. Chen, C. G. Shi, D. H. Cao, H. J. Ying, and X. Q. Wang, "Control of post-construction settlement by replacing subgrade with foamed cement banking," *Chinese Journal of Geotechnical Engineering*, vol. 33, no. 12, pp. 1854–1862, 2011.

[31] Q. Z. Jiang, Z. P. Chen, J. B. Wang, and J. F. Liu, "the method of determining the thickness of foamed cement banking," *Highway*, vol. 4, pp. 84–88, 2019.

[32] C. B. Crawford, "Interpretation of the consolidation test," *Soil Mechanics and Foundation Division Journal*, vol. 90, no. 5, pp. 87–102, 1964.

[33] Z. Y. Liu and Z. L. Zheng, "Estimation of reference time in EVP model," *Chinese Journal of Underground Space and Engineering*, vol. S1, no. 14, pp. 134–139, 2018.